OPTIMIZING PROCESSES USING RESPONSE SURFACE METHOD FOR THE PHOTODEGRADATION OF A SYNTHESIZED DISPERSE DYE DERIVED FROM 2-AMINO-4-METHYL-5-CARBATHOXYTHIAZOLE

DANLADI, E.*, **GIWA, A. AND NKEONYE, O.P.**
Department of Textile Science and Technology, Ahmadu Bello University, Zaria, Nigeria

ABSTRACT

Response surface methodology (RSM) is an extensively used method designed for modeling and optimization of photocatalytic treatment processes of water and wastewater. In this study, photocatalytic degradation of a synthesized azo disperse dye, under UV light irradiation using TiO_2 (P25) as photocatalyst in a prototype cylindrical reactor was studied. The RSM was employed to assess individual and interactive effects of four main independent parameters such as initial dye concentration, catalyst load, pH, and irradiation time on the percentage degradation. Central Composite Design was used for optimization of UV/TiO_2 process. Predicted values of degradation (%) were found to be in good agreement with experimental values, which showed R^2 of 84.12 and Adj-R^2 of 70.22 for the synthesized dye. Optimization results showed that optimum percentage degradation was achieved at the following optimum conditions: initial dye concentration of 30.0 mg/L, catalyst load of 0.0937 g/L, pH of 10.3 and irradiation time of 132.845 min. The results showed that RSM can describe the behavior of complex reaction systems in the range of experimental conditions adopted. Optimization based on RSM can also estimate the conditions of the photocatalytic processes to achieve the highest performance.

Keywords: TiO_2, photocatalysis, degradation, dispersed dye.
***Correspondence**: danladielijah@yahoo.com

INTRODUCTION

Still in some recent studies, only traditional one-factor-at-a-time experiments were used for evaluating the effects of operating factors on the photocatalytic process efficiency. This practice is not only time and work demanding, but also totally deficient in representation of the effect of interaction amongst different factors i.e. experiments are carried out by varying systematically, the studied parameter and keeping the others constant and vice-versa, resulting in an unreliable number of experiments. In this way, the information about the relation between factors and response are not obtained in an empirical way [1, 2, 3]. By using RSM, it is conceivable to estimate linear interaction and quadratic effects of the factors and to provide a forecast model for the response. RSM allows a suitable design of the experiments, which assists to reduce the number of runs. More so, the modeling of the system simplifies the interpretation of multivariate phenomena and is a valuable tool for scaling up [4].

Treatment of hazardous industrial effluents is one of the growing needs of the present time. Advanced Oxidation Processes (AOPs) have been developed to convert nonbiodegradable contaminants into harmless products [5, 6, 7]. Heterogeneous photocatalysis, a novel process belonging to the class of AOPs, via combination of photocatalysts, such as TiO_2 and ultraviolet (UV) light, is an attractive alternative treatment method for the removal of toxic pollutants from wastewater, owing to its ability to degrade the pollutants into innocuous end-products, such as CO_2, H_2 and mineral acids [8, 9]. The preferential use of TiO_2 for the photocatalytic degradation of organic pollutants is based on its availability, low cost and photochemical stability [10].

Population growth increases the environmental load irrespective of the rate of economic growth, because the rapid urbanization has its effects on pollution of river systems and creation of solid wastes [11]. The usage of water is increasing day by day due to the increasing number of chemical industries. Of all the chemical industries, the textile industries are one of the major water consuming industries and a major source of environmental pollution [12]. In these industries, water is used with different chemicals and auxiliaries, which are used for producing textile goods [13]. Approximately, more than 10,000 different dyes and pigments are in industrial use, representing the annual consumption of around 700,000 tones worldwide [14].

Environmental pollution on a global scale, as well as the lack of sufficient clean energy sources, have drawn much attention to the need for developing ecologically clean chemical technology, materials and process [15]. Azo dyes, being the largest group of synthetic dyes, represent up to 70% of all the known commercial dyes produced. In recent years, research in new non-biological methods has led to processes which actually destroy these pollutants instead of simply extracting them from water [16-20].

This study is therefore aimed at synthesizing an azo disperse dye and subjecting the dye to photodegradation using RSM for the optimization of the degradation factors for maximum efficiency.

MATERIALS AND METHODS

Materials

Resublimed iodine, iodine, ethylacetoacetate, thiourea, ammonium hydroxide, sulphuric acid, sodium nitrite, acetic acid, starch iodide paper, H-acid, sulphamic acid, sodium hydroxide, methylated spirit, N, N-dimethylaniline, hydrochloric acid, filter paper, Degussa P25-TiO_2,

Equipment

Mercury bulb (25W) B22, 220-240V black light, Jenway UV-Visible Spectrophotometer; Model:6305, Digital pH Meter, hot plate/magnetic stirrer, electronic weighing balance, Shimadzu FTIR-8400S Fourier Transform Infrared Spectrophotometer, photo reactor equipped with heat suction fan (Model 3610KL-04W-B69,12V DC,0.56A, DC Brushless, MINEBEA CO., LTD Made in China) and a UV bulb (25W) stated above.

Synthesis of intermediate Preparation of 2-amino-4-methyl-5-carbathoxythiazole

Resublimed iodine (7.6 g, 0.03 mol) was added to a slurry of ethylacetoacetate (3.9 g, 0.03 mol) and thiourea (4.56 g, 0.06 mol) and the mixture was heated in an oil bath of glycerol at 130-140°C overnight. After being cooled, the reaction mixture was diluted with distilled water (50 ml) and heated to dissolve most of the solid, then cooled to ambient temperature and treated with 25% ammonium hydroxide to pH 9. The precipitated thiazole was collected and purified by re-crystallization from hot ethanol. The yield was determined and the FTIR spectral analysis was also carried out.

Diazotization for the disperse dyes

Sodium nitrite (0.83 g, 0.012 mol) was added to concentrated sulphuric acid (98%, 11.76 g, 0.12 mol) at 30°C. The mixture was heated to 60-65°C and stirred over 15 minutes and maintained at this temperature for 30 minutes to ensure complete dissolution of $NaNO_2$. The mixture was cooled to 5°C, and then concentrated acetic acid (5 ml) added and stirred for 10 minutes. The temperature was reduced to between 2-5°C and then the appropriate aminothiazole (0.012 mol) added for over 30 min. The reaction mixture was stirred at the same low temperature for 2 hr. Completion of the diazotization was confirmed using starch iodide paper for the presence of excess of nitrous acid.

Coupling for the synthesis of disperse dye

Solution of equimolar quantities of the coupling component N, N-dimethylaniline (0.48 g, 0.004 mol) was prepared by dissolving the N,N-dimethylaniline in a mixture of hydrochloric acid (1.5 ml) and ice water (40 ml). The diazo solution was added gradually with stirring and the mixture buffered with sodium hydroxide to pH 4. The stirring continued for 2 hr and then the product was filtered off and washed thoroughly with water and dried.

Synthesis of Disperse dye

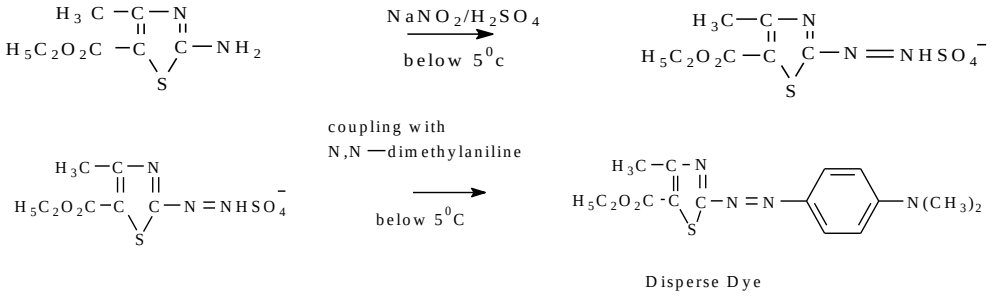

Scheme 1: Synthesis of disperse dye from N, N- dimethylaniline and 2-amino-4-methyl-5-carbathoxythiazole

Photodegradation experiment

Before the degradation experiment, the synthesized dye was purified repeatedly by recrystallization, followed by filtration and drying. The peak of maximum absorption wavelength (λ_{max}) for the dye was determined in ethanol using Jenway UV/Visible Spectrophotometer.

The photocatalytic degradation reaction was carried out using the photoreactor (Fig. 1) equipped with a 25W mercury bulb, B22, 220-240V (China) and a suction fan (Model 3610KL-04W-B69, 12V DC, 0.56A, DC Brushless, MINEBEA CO., LTD China) fixed directly above the reactor (400ml beaker) containing the dye solution followed by the switch being turned on to power the fan as well as the magnetic stirrer and the bulb.

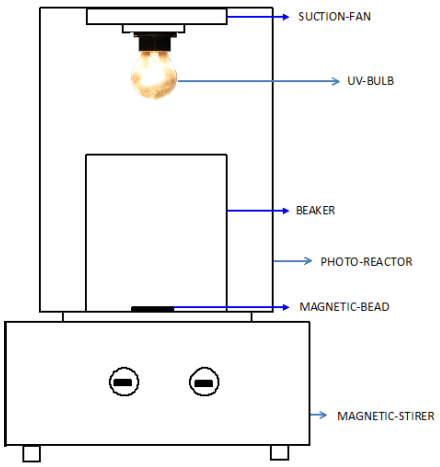

Fig. 1: Photoreactor

Determination of pH

The pH was determined with a digital pH meter at room temperature after standardizing with buffer solutions of pH 7 and 4. The electrode was then dipped into the sample and the value was recorded.

Experimental Design

Experimental design, Central Composite Design was carried out using Minitab 16 software based on operational parameters: dye concentration, catalyst load, pH of solution, and time of exposure for the disperse dye. All experiments were carried out using deionized water. The experimental ranges for each of the operational parameters are shown in Table 1:

Table 1: Experimental ranges and levels of the independent test variables

Factor	Name	Low	High
A	Dye concentration (mg/L)	0	20
B	Catalyst load (g/L)	0	2
C	pH	4.3	8.3
D	Time (min)	0	90

Factors: 4; Blocks: none; Center points in cube: 7; Runs: 31; Alpha: 2; Center points in star: 0

The solutions were made by preparing a 40 mg/L of the dye and 100 ml of the required concentration prepared by serial dilution from the stock solution and adjusting the pH using dilute HCl and dilute NaOH solutions based on the design followed by placing the solution in the photo reactor to expose the dye solution to the UV light where necessary. After each reaction time, an aliquot was withdrawn using a 5 ml syringe fitted with 0.2 µm nylon filter. Absorbance readings were taken at the start of the experiment before irradiation $(Absorbance)i$ and after irradiating for time t $(Absorbance)f$.

$$\text{Degradation (\%)} = \frac{(Absorbance)i-(Absorbance)f}{(Absorbance)i} \times 100$$

RESULTS AND DISCUSSION

The wavelength of maximum absorption of the synthesized disperse dye was determined in ethanol using Jenway UV-Vis Spectrophotometer and was found to be 532 nm. The molecular weight, % yield and IR peaks was determined for the dye and the results are as shown in Table 2.

Table 2: Dye structure and physical properties

Structures	M.Wt	Yield (%)	IR Peaks (cm^{-1})
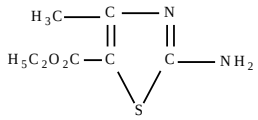 **Intermediate**	186	33.5	NH at 3433,162 at 2942, 3043, 3191
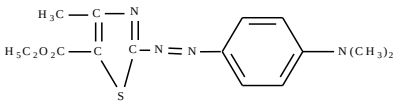 **Disperse dye**	318	79.6	CC at 1396, CN at 1314, CS at 597, 643, CO at 1132, CH_3 at 1363, NH at 1621, 3357, CH at 788

Response Surface Methodology

Table 3: Design of experiment

Run Order	Dye Concentration (mg/L)	Catalyst load (g/L)	pH	Time (min)	Absorbance $C_{initial}$	Absorbance C_{final}	Degradation (%)
1	20	0	8.3	0	0.040	0.040	0.000
2	10	1	6.3	45	0.046	0.023	50.000
3	0	0	4.3	90	0.096	0.095	1.040
4	0	0	8.3	90	0.095	0.085	10.530
5	10	1	6.3	45	0.031	0.018	41.940
6	20	2	8.3	0	0.016	0.016	0.000
7	20	0	8.3	90	0.037	0.013	64.870
8	20	0	4.3	90	0.036	0.012	66.670
9	10	3	6.3	45	0.040	0.013	67.500
10	10	1	10.3	45	0.045	0.014	68.890
11	10	1	6.3	135	0.039	0.005	87.180
12	30	1	6.3	45	0.037	0.013	1.050
13	20	0	4.3	0	0.014	0.014	0.000
14	0	2	8.3	90	0.092	0.088	4.350
15	10	1	6.3	45	0.046	0.023	50.000

Run Order	Dye Concentration (mg/L)	Catalyst load (g/L)	pH	Time (min)	Absorbance $C_{initial}$	Absorbance C_{final}	Degradation (%)
16	10	1	6.3	45	0.046	0.023	50.000
17	0	2	4.3	90	0.095	0.092	3.160
18	0	0	4.3	0	0.001	0.001	0.000
19	20	2	8.3	90	0.041	0.024	41.460
20	10	1	6.3	45	0.046	0.023	50.000
21	0	2	8.3	0	0.019	0.019	0.000
22	0	2	4.3	0	0.019	0.019	0.000
23	10	1	6.3	45	0.046	0.023	50.000
24	20	2	4.3	0	0.017	0.017	0.000
25	10	1	6.3	45	0.046	0.023	10.000
26	20	2	4.3	90	0.095	0.077	18.950
27	10	1	6.3	45	0.046	0.023	50.000
28	10	1	2.3	45	0.094	0.094	0.000
29	10	1	6.3	45	0.046	0.023	50.000
30	0	0	8.3	0	0.018	0.018	0.000
31	10	1	6.3	45	0.046	0.023	50.000

The adequacy of a model is evaluated by the residuals (difference between the observed and the predicted response value). Residuals are thought as elements of variation unexplained by the fitted model and then it is expected that they occur according to a normal distribution. Normal probability plots are suitable graphical methods for judging residual normality [22]. Therefore, in this study, the observed residuals are plotted against the expected values, given by a normal distribution (Figs. 2 – 5). The trends reveal reasonably well-behaved residuals. Based on these plots, the residuals appear to be randomly scattered.

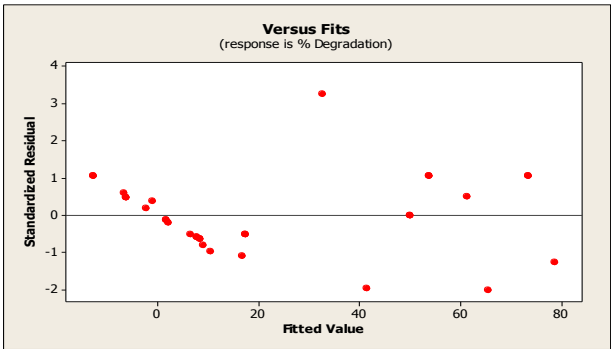

Fig. 2: Standardized residual versus fitted value

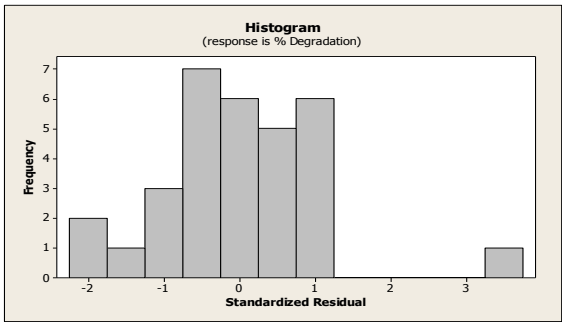

Fig. 3: Histogram of frequency versus standardized residual

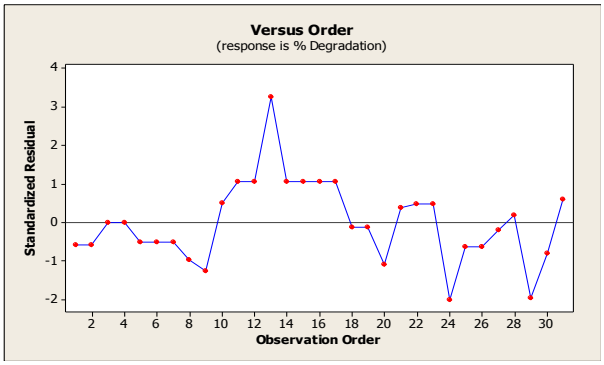

Fig. 4: Standardized residual versus observation order

The plot presented in Fig. 4 tests the assumption of constant variance. The points are randomly scattered and all values lie within the range of −2.19 and 3.4 (values between −3 and +3 are considered as the top and bottom outlier detection limits). According to the layouts of the plots presented in Fig. 4, it was concluded that used response transformation was appropriate, that there was no apparent problem with normality.

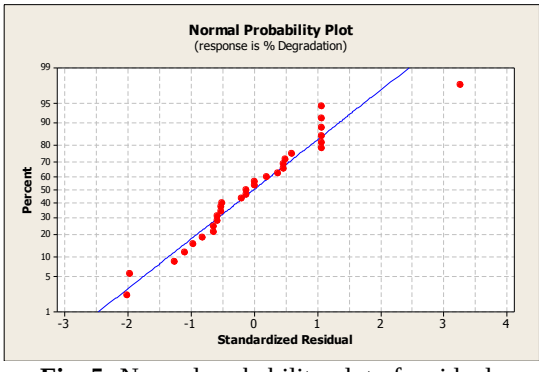

Fig. 5: Normal probability plot of residuals

The high correlation between observed and predicted data can be seen from the graphical interpretation given in Fig. 5. It is evident that the points or point clusters are placed very closely to the diagonal line as a result of their low

discrepancies. This observation leads to the conclusions that there are no serious violations in the assumptions that errors are normally distributed and independent of each other that the error variances are homogeneous and that residuals are independent.

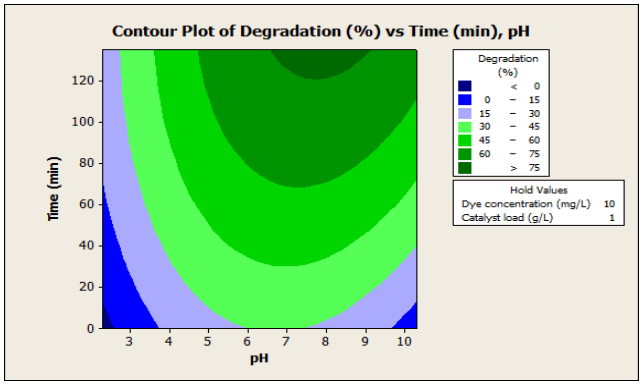

Fig. 6: Contour plot of % degradation versus time, pH

Figure 6 gives an insight to where and when degradation is actually taking place and also indicates that as the irradiation time increases, there is a steady increase in degradation. As the pH increases, the degradation also increases, until when the pH approaches 7.5, before degradation is observed to be decreasing. This could be attributed to the fact that the surface activity of the photo catalyst is affected by an alkaline pH. But higher irradiation time influences the photo catalysis, hence higher % degradation. It can be concluded that the degradation is better between pH 7 and 8 for dye concentration of 10 mg/L and catalyst load of 1 g/L, and for time ranging from 120-140 min.

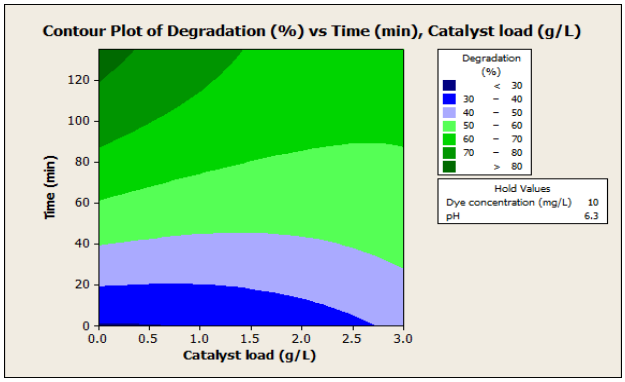

Fig. 7: Contour plot of % degradation versus time and catalyst load

The Fig. 7 is also a contour plot that illustrates the variation of % degradation with respect to irradiation time but with catalyst load. As the irradiation increases, there is a steady increase in degradation. The catalyst load also influences the % degradation progressively. This is true for dye concentration of 10mg/L and pH of 6.3. at 120 minutes irradiation time, however, less than 0.5mg/L of the catalyst is needed to achieve a degradation above 80%.

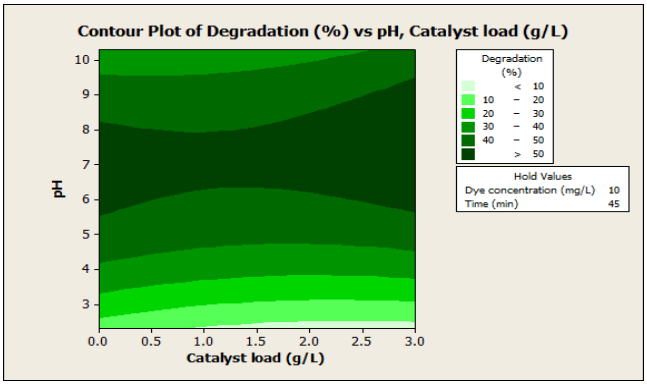

Fig. 8: Contour plot of % degradation versus pH and catalyst load

Figure 8 shows the effect of pH and catalyst load for the synthesized disperse dye. At dye concentration of 10 mg/L and irradiation time of 45 min, the % degradation increases as pH increases and attains maximum between pH 5.5 and 8.3. The catalyst load also influences the % degradation in like manner. But as the catalyst load increases, beyond 1.5 g/L, there is a downward trend in the % degradation. This implies that the % degradation of greater than 50% is achievable provided that pH is between 5.5 and 8.3 and a catalyst load of 1.5 respectively.

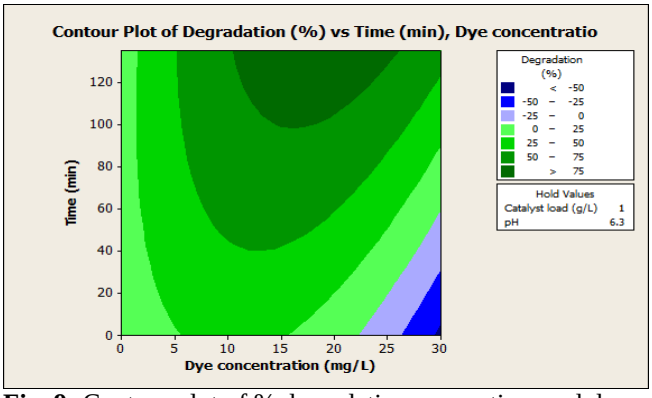

Fig. 9: Contour plot of % degradation versus time and dye concentration

Figure 9 illustrates the effect of irradiation time and dye concentration at catalyst load of 1 g/L and pH of 6.3 respectively for disperse dye. As the irradiation time increases, there is a corresponding increase in % degradation. As dye concentration increases degradation also increases up to 22.5 mg/L before it starts to decrease progressively. This is because the higher the concentration the longer time it takes for the light to penetrate the dye molecule. For the above condition, better result is achieved at dye concentration of 15 mg/L and irradiation time of 100 to 120 min respectively.

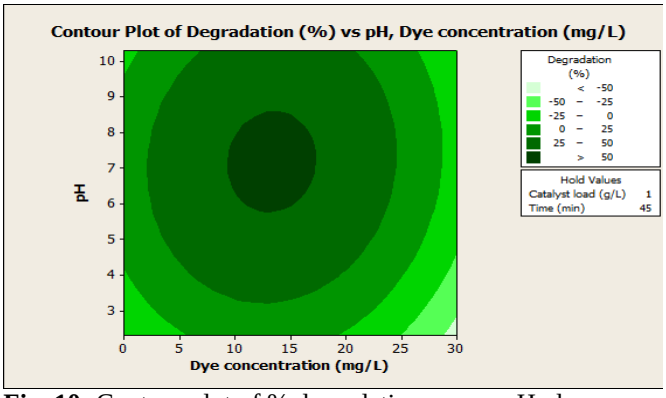

Fig. 10: Contour plot of % degradation versus pH, dye concentration

Figure 10 illustrates the effect of pH and dye concentration at catalyst load of 1 g/L and irradiation time of 45 min for the dye. The % degradation increases steadily as the pH increases. As the dye concentration increases there is also an increase in % degradation until it reaches 15 mg/L before it starts decreasing steadily. This implies that as the pH and dye concentration increases there is a corresponding increase in % degradation with the best result being at dye concentration of 15mg/L and pH of 6-8.5 respectively. pH and dye concentration play a role in degradation at catalyst load of 1 g/L and irradiation time of 45 min. Increase in the pH enhances the degradation with exception of any pH less than 5.5 and greater than 12.

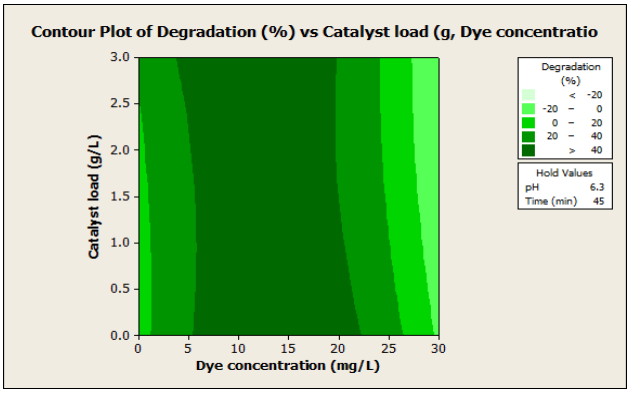

Fig. 11: Contour plot of % degradation versus catalyst load and dye concentration

Figure 11 shows the effect of catalyst load and dye concentration for pH of 6.3 and irradiation time of 45 minutes respectively. This show that % degradation increases as dye concentration increases until it begins to approach 22.5 mg/L where it starts dropping and the catalyst load is at 2.5-3 mg/L. This implies that the catalyst load has effect when it is 2.5 mg/L and 3 mg/L.

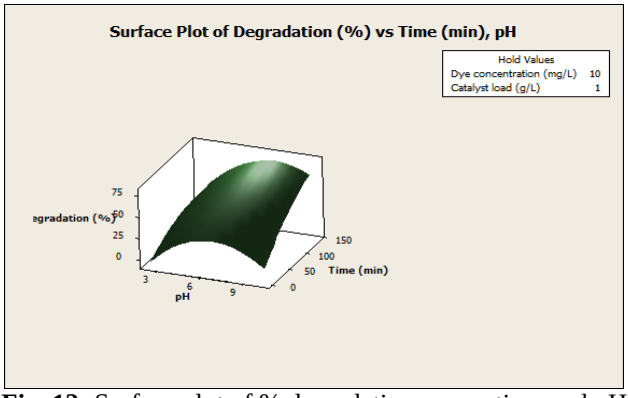

Fig. 12: Surface plot of % degradation versus time and pH

The surface plot Fig. 12 illustrates the changes in % degradation with respect to pH and irradiation time in three dimensional views at dye concentration and catalyst load of 1 g/L. the plot above shows that as the pH increases there is a steady increase in % degradation until slightly above 6 before it begins to decrease. For the irradiation, there is an increase in % degradation as irradiation time increases steadily.

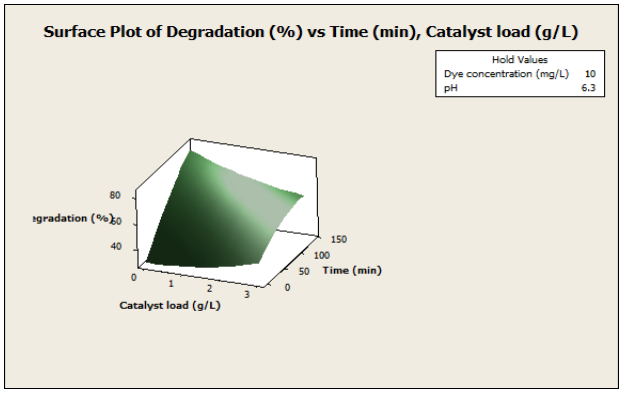

Fig. 13: Surface plot of % degradation versus time and catalyst

The three dimensional views in Fig. 13, illustrates the effect of catalyst load and irradiation time at dye concentration of 10 mg/L and pH of 6.3 respectively. The views show that there is steady increase in degradation as the catalyst load as well as the irradiation time increase.

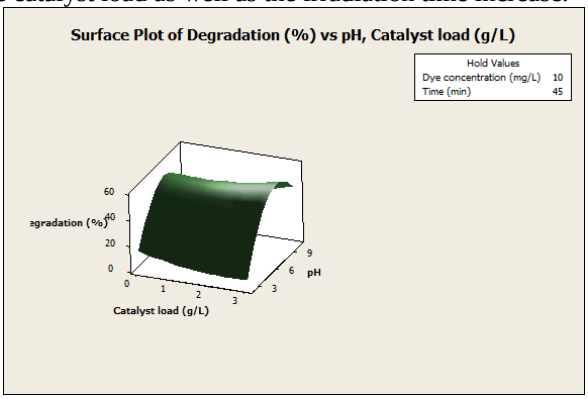

Fig. 14: Surface plot of % degradation versus pH and catalyst load

Figure 14 shows that % degradation increases steadily as pH and catalyst load increase at dye concentration of 10 mg/L and irradiation time of 45 minutes but as the pH exceeds 7, there is a downward trend in % degradation. This implies that the % degradation decreases at strongly alkaline pH.

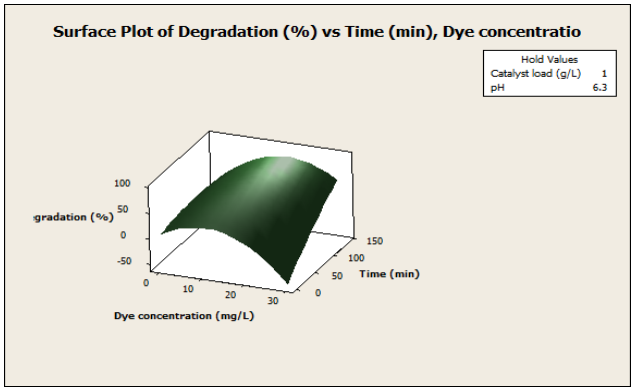

Fig. 15: Surface plot of % degradation versus time and dye concentration

Figure 15 shows the effects of dye concentration and irradiation time. The views show that % degradation increases with increase in irradiation time but as dye concentration increases, there is a downward trend in % degradation from 20 mg/L. this also shows that dye concentration affect the % degradation of the dye.

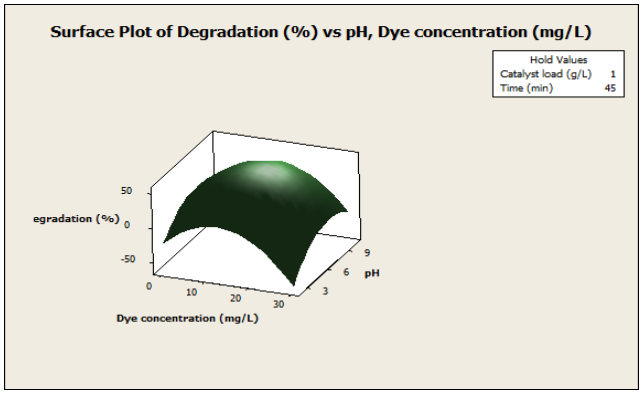

Fig. 16: Surface plot of % degradation versus pH and dye concentration

Figure 16 shows the effect of dye concentration and pH on % degradation at catalyst load of 1 g/L and irradiation time of 45 min, % degradation increases with increase in dye concentration and pH but as the pH and dye concentration reach a certain value, the % degradation decreases i.e. from dye concentration of 20 mg/L and pH of 6.3 respectively.

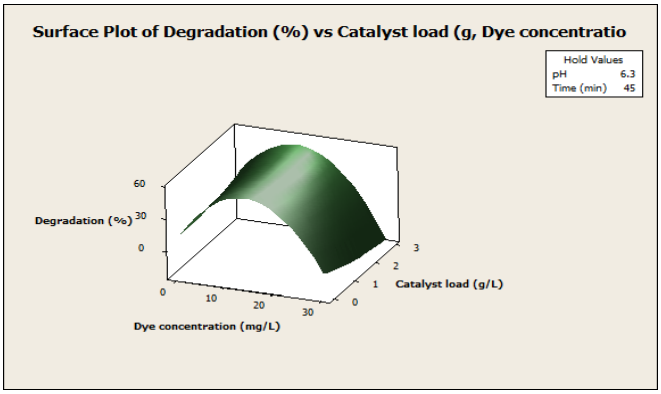

Fig. 17: Surface plot of % degradation versus catalyst load and dye concentration

The views above Fig. 17 show that dye concentration and catalyst load have effects on % degradation at pH of 6.3 and irradiation time of 45 min. As the dye concentration reaches 20 mg/L there is a downward trend in % degradation.

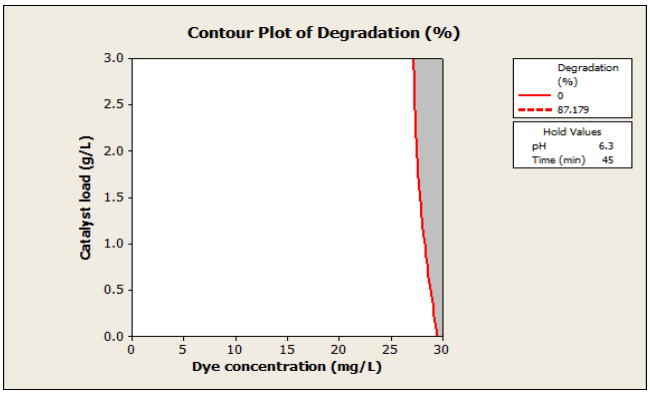

Fig. 18: Contour plot of % degradation

Figure 18 shows the feasibility of degradation at pH of 6.3 and irradiation time of 45 minutes, this implies that as the dye concentration approaches 30 mg/L, the degradation becomes almost impossible. But the catalyst load does not affect the degradation negatively. This shows that degradation is possible up to concentrations close to 30 mg/L.

Optimal conditions

The optimal values of the dependent variables in the photodegradation system were determined. The experimental conditions for maximum dye removal (85%) were 30 mg/L for the dye concentration, catalyst load of 0.09, pH of 10.3 and exposure time of 132.845 min, however, low error of 0% and low standard deviation of 0% was achieved for the response. An experimental test was conducted using the predicted values. The experimental findings the response parameter was in close agreement with the model predictions indicating complete dye removal.

CONCLUSION

From the above studies, it can be concluded that RSM describes the behaviour of the complex reaction system, such as photocatalytic processes in the range of experimental conditions adopted. Optimization based on RSM can estimate the conditions of the photocatalytic processes in order to achieve highest performance. This methodology provides a prediction model for the response for the range of variables studied and the optimum conditions in order to achieve the highest performance.

REFERENCES

1. BROWN, S. TAULER, R & WALCZAK, R. (2009). Comprehensive Chemometrics, Vol. 1, Elsevier, Amsterdam, pp. 345–390.
2. SANTOS, S.C.R. & BOAVENTURA, R.A.R. (2008). Adsorption modeling of textile dyes by sepiolite, *Applied Clay Science*. **42**, 137-145.
3. MYERS, R.H. & MONTGOMERY, D.C. (2002). Response Surface Methodology Process and Product Optimization using Designed Experim - ents. John Wiley & Sons, Inc., New York. USA.
4. BRAUN, A.M. JAKOB, L., OLIVEROS, E. & DO NASCIMENTO, C.A.O. (2007). Up-Scaling Photochemical Reactions, John Wiley & Sons, Inc., Hoboken, New Jersey, USA, pp. 235-313.
5. GALINDO, C. JACQUES, P. & KALT, A. (2001). Photooxidation of the phenylazonaphthol on TIO_2: kinetic and mechanistic investigations, *Chemosphere*, **45**, 997-1005.
6. DANESHVAR, N. & KHATAEE, A.R. (2006). Removal of Azo Dye C.I. Acid Red 14 from contaminated water using Fenton, UV/H_2O_2,UV/H_2O_2/Fe(II), UV/H_2O_2/Fe(III) and UV/H_2O_2/Fe(III)/oxalate processes: a comparative study, *Journal of Environmental Science and Health*, Part A, **41:** 315-328.
7. DANESHVAR, N., SALARI, D., NIAEI, A. & KHATAEE, A.R. (2006). Photocatalytic degradation of the herbicide erioglaucine in the presence of nanosized titanium dioxide: comparison and modeling of reaction kinetics, *Journal of Environmental Science and Health*, Part B, **41**: 1273-1290.
8. KHATAEE, A.R., ALEBOYEH, H. & ALEBOYEH, A. (2009). Crystallite phase-controlled preparation, characterisation and photocatalytic properties of titanium dioxide nanoparticles, *Journal of Experiments in Nanoscience*, **4**, 121-137.
9. KHATAEE, A.R. VATANPOUR, V. & AMANI GHADIM, A. R. (2009) Decolorization of C.I. Acid Blue 9 solution by UV/Nano-TiO_2, Fenton, Fenton-like, electro-Fenton and electrocoagulation processes: a comparative study, *Journal of Hazardous Materials*, **161:** 1225-1233.
10. SIN, J.C., LAM, S. M. & MOHAMED, A. (2011). Optimizing photocatalytic degradation of phenol by TiO_2/GAC using response surface methodology, *Korean Journal of Chemical Science and Engineering*, **28**: 84-92.
11. GRIMM, B.N., FAETH1, H.S., GOLUBIEWSKI, E. N., CHARLES, L.R., JIANGUO W., XUEMEI B., & JOHN, M.B. (2008). Global Change and the Ecology of Cities. *Science*, **319** (5864): 756-760. DOI: 10.1126/science.1150195.
12. REN, X. (2000). Development of environmental performance indicators for textile process and product, *Journal of Cleaner Production*, **8**: 473-481
13. SHISHOO, R.L. (1994). Environmental issues facing the technical textile industry in Europe. *Journal of Industrial Textiles*, **24**: 117-128
14. AKHTAR, S, KHAN A.A, & HUSAIN Q. (2005). Partially purified bitter gourd (Momordica charantia) peroxidase catalyzed decolorization of textile and other industrially important dyes. *Bioresource Technology*, **96**:1804-11.
15. ABO-FARHA, S.A. (2010). Photocataltic degradation of monoazo and disazo dyes in wastewater on nanometer-sized TiO_2. *Journal of American Science*, **6** (11): 130-142
16. DEHGHANI, M.H., JAAFARI, J., ALGHAS, A., & PORKAR, G. (2011). Using medium pressure ultraviolet reactor for removing azo dyes in textile wastewater treatment plant. *World Applied Sciences Journal*, **12** (6):.797-802.
17. GIWA, A., NKEONYE, P.O., BELLO, K.A. & KOLAWOLE, E.G. (2011a).Solar Photocatalytic Degradation of Acid Blue 29. *Journal of the Chemical Society of Nigeria*, **36** (1): 82-89.
18. GIWA, A., AKPAN, U.G., NKEONYE, P.O., BELLO, K.A. & KOLAWOLE, E.G. (2011b). Decolourization and Mineralization of Reactive Violet 1 by UV-Photolysis in the presence of hydrogen peroxide. *Nigerian Journal of Material Science and Engineering*, **2**(1): 80-89.
19. KHAVITHA, S.K., & PALANISAMY, P.N. (2011). Photocatalytic and sonophotocatalytic degradation of Reactive Red 120 using dye sensitized TiO_2 under visible light. *International journal of Civil and environmental Engineerin*, **3** (1): 1-6.
20. MALARVIZHI, R., WANG, M. & HO, Y. (2010). Research trends in adsorption technologies for dye containing wastewater. *World Applied Sciences Journal*, **8** (8): 930-942.
21. Minitab 16 software
22. Stat-Ease, 2008